

Optimal path of diffusion over the saddle point and fusion of massive nuclei

Chun-Yang Wang,¹ Ying Jia,² and Jing-Dong Bao^{1,3*}

¹*Department of Physics, Beijing Normal University, Beijing 100875, China*

²*College of Science, The Central University for Nationalities, Beijing 100081, China*

³*Center of Theoretical Nuclear Physics, National Laboratory of Heavy-ion Accelerator, Lanzhou 730000, China*

(Dated: November 14, 2018)

Diffusion of a particle passing over the saddle point of a two-dimensional quadratic potential is studied via a set of coupled Langevin equations and the expression for the passing probability is obtained exactly. The passing probability is found to be strongly influenced by the off-diagonal components of inertia and friction tensors. If the system undergoes the optimal path to pass over the saddle point by taking an appropriate direction of initial velocity into account, which departs from the potential valley and has minimum dissipation, the passing probability should be enhanced. Application to fusion of massive nuclei, we show that there exists the optimal injecting choice for the deformable target and projectile nuclei, namely, the intermediate deformation between spherical and extremely deformed ones which enables the fusion probability to reach its maximum.

PACS numbers: 24.10.-i, 24.60.-k, 25.70.Jj, 05.20.-y

I. INTRODUCTION

The saddle point passage problem is of great interest in various fields of physics, such as collision of molecular systems, atomic clusters, biomolecules, and so on. The previous studies on this issue were mostly concentrated on a simple diffusive dynamics with single degree of freedom, where the Langevin equation with constant coefficients can be easily solved in the case of a quadratic potential [1]. However, since many processes obviously involve more than one degree of freedom, which the one-dimensional (1D) model does not distinctly hold, high dimension at least two dimension (2D) is necessary. A case in point would be the fusion reaction of massive nuclei, where the fusion is induced by diffusion [2, 3] and the asymmetrical or the neck degree of freedom of compound nuclei needs to be considered [4, 5]. For these systems with the contact point of two colliding nuclei being very close to the conditional saddle point, the potential energy surface (PES) around the saddle point can be approximated to be a quadratic type. Under this approximation, Abe *et al.* [6] obtained an analytical expression for the multi-dimensional saddle-point passing probability. Some authors discussed quantum effect of the fusion probability by using the real time path integral [7] or the quantum transport equation [8, 9], respectively. Boilley *et al.* [10] studied the influence of initial distribution upon the passing probability. Anomalous diffusion passing over the saddle point of 1D quadratic potential was also discussed in Ref. [11]. Nevertheless, it is not completely clear for the dynamical role of non-transport degrees of freedom. This might be very important for the quasi-fission mechanism in the fusion reaction, because the average path of the fusing system in a multi-dimensional PES should be controlled by the off-diagonal

components of inertia and friction tensors before the system arrives firstly at the conditional saddle point.

Recently, theoretical calculations for the fusion barrier distribution, accounting for the surface curvature correction to the nuclear potential, have been presented by Hinde *et al.* [12, 13, 14]. The geometrical effect significantly changes the near-barrier fusion cross section and the shape of the barrier distribution through an angle-dependent potential, where the target nucleus bears quadrupole and hexadecapole deformations while the projectile one is in a spherical shape. In these calculations, the surface curvature correction to the sphere-to-sphere nuclear potential exerts influences upon the fusion probability through the height of fusion barrier. However, the dynamical coupling effect of various deformative degrees of freedom needs to be added from the viewpoint of fusion by diffusion [3].

The primary purpose of this paper is to study the influence of coupling between two degrees of freedom upon the passing probability. In Sec. II, we report the analytical expression of the saddle-point passing probability by solving the 2D coupled Langevin equation with constant coefficients. In Sec. III, we discuss the effects of off-diagonal components of inertia, friction and potential-curvature tensors and then determine the optimal diffusive path. Sec. IV gives an application of this study to the actual fusion process of massive nuclei. A summary is written in Sec. V.

II. THE PASSING PROBABILITY

We consider the directional diffusion of a particle in a 2D quadratic PES: $U(x_1, x_2) = \frac{1}{2}\omega_{ij}x_ix_j$ with $i, j = 1, 2$ and $\det \omega_{ij} < 0$, the motion of the particle is described by the Langevin equation

$$m_{ij}\ddot{x}_j(t) + \beta_{ij}\dot{x}_j(t) + \omega_{ij}x_j(t) = \xi_i(t) \quad (1)$$

*Corresponding author. Electronic mail: jdbao@bnu.edu.cn

with $x_j(0) = x_{j0}$ and $\dot{x}_j(0) = v_{j0}$, where $x_{10} < 0$ and $v_{10} > 0$. Here and below the Einstein summation convention is used. The two components of the random force are assumed to be Gaussian white noises and their correlations obey the fluctuation-dissipation theorem $\langle \xi_i(t)\xi_j(t') \rangle = k_B T m_{ik}^{-1} \beta_{kj} \delta(t-t')$, where k_B is the Boltzmann constant and T the temperature.

Assuming that x_1 -axis is the transport direction [$\omega_{11} < 0$], we write the reduced distribution function of the particle for x_1 while the variables $x_2(t)$, $v_1(t)$ and $v_2(t)$ are integrated out,

$$W(x_1, t; x_{10}, x_{20}, v_{10}, v_{20}) = \frac{1}{\sqrt{2\pi}\sigma_{x_1}(t)} \exp\left(-\frac{(x_1(t) - \langle x_1(t) \rangle)^2}{2\sigma_{x_1}^2(t)}\right). \quad (2)$$

Integrating over x_1 from zero to infinity, we determine the passing probability over the saddle point [$x_1 = x_2 = 0$] as

$$P(t; x_{10}, x_{20}, v_{10}, v_{20}) = \int_0^\infty W(x_1, t; x_{10}, x_{20}, v_{10}, v_{20}) dx_1 = \frac{1}{2} \operatorname{erfc}\left(-\frac{\langle x_1(t) \rangle}{\sqrt{2}\sigma_{x_1}(t)}\right). \quad (3)$$

Applying the Laplace transform technique to Eq. (1), we thus get $x_1(t)$ and its variance $\sigma_{x_1}^2(t)$ at any time,

$$x_1(t) = \langle x_1(t) \rangle + \sum_{i=1}^2 \int_0^t H_i(t-t') \xi_i(t') dt', \quad (4)$$

$$\sigma_{x_1}^2(t) = \int_0^t dt_1 H_i(t-t_1) \int_0^{t_1} dt_2 \langle \xi_i(t_1)\xi_j(t_2) \rangle H_j(t-t_2), \quad (5)$$

where the mean position of the particle along the transport direction is given by

$$\langle x_1(t) \rangle = \sum_{i=1}^2 [C_i(t)x_{i0} + C_{i+2}(t)v_{i0}], \quad (6)$$

which relates to the initial position and velocity. The time-dependent factors in Eq. (6) with exponential forms according to the residual theorem are $C_i(t) = \mathcal{L}^{-1}[F_i(s)/P(s)]$ ($i = 1 \dots 4$), the two response functions in Eqs. (4) and (5) read $H_1(t) = \mathcal{L}^{-1}[F_5(s)/P(s)]$ and $H_2(t) = \mathcal{L}^{-1}[F_6(s)/P(s)]$, where \mathcal{L}^{-1} denotes the inverse Laplace transform. The expressions of $P(s)$ and $F_i(s)$ ($i = 1, \dots, 6$) are written in the appendix.

III. THE OPTIMAL DIFFUSIVE PATH

A. The coupling effect of two degrees of freedom

As one has known in the 1D case, the passing probability increases from 0 to 1 when the initial velocity of

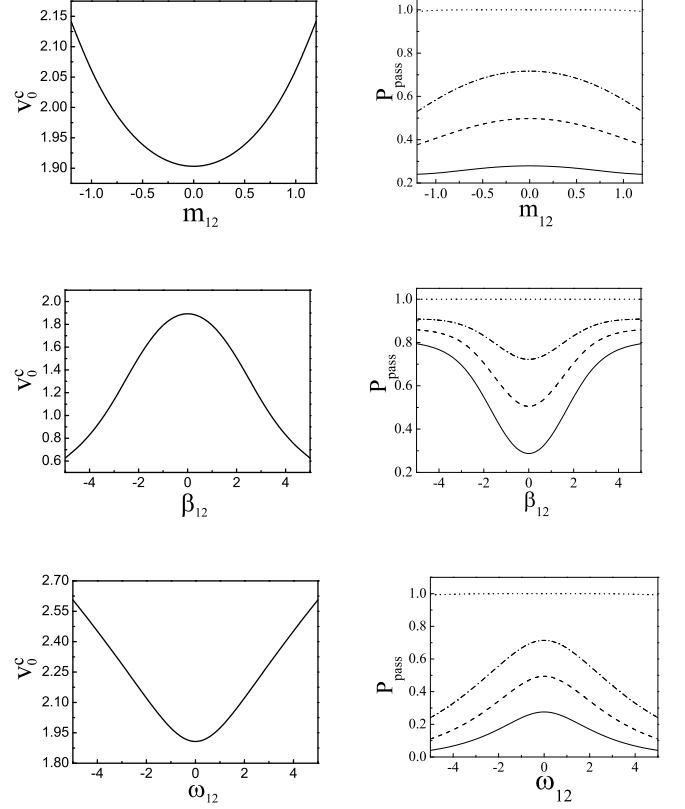


FIG. 1: The critical velocity (left) and the stationary passing probability (right) as functions of various off-diagonal components m_{12} , β_{12} , and ω_{12} , respectively. The parameters used are: $m_{11} = 1.5$, $m_{22} = 2.0$, $\beta_{11} = 1.8$, $\beta_{22} = 1.2$, $\omega_{11} = -2.0$, $\omega_{22} = 1.5$, and $\theta = 0$. The initial velocities of the particle are $v_0 = 4.0, 2.2, 1.9, 1.6$ from top to bottom (right).

the particle increases. The critical velocity is defined by the passing probability being equal to $\frac{1}{2}$. This leads to the condition: $\lim_{t \rightarrow \infty} \langle x_1(t) \rangle = 0$. If all the off-diagonal components of the three coefficient tensors are not considered, as well as x_{20} and v_{20} are taken to be zero, the critical velocity is determined from Eq. (6): $v_0^c = [F_1(a)/F_3(a)]x_{10}$, where a is the largest positive root of $P(s) = 0$. This is in fact identical to the one-dimensional result: $v_0^c = -x_{10}(\sqrt{\beta_{11}^2 + 4\omega_{11} + \beta_{11}})/(2m_{11})$ [6], which is proportional to the friction strength.

We now consider all the off-diagonal components of three coefficient tensors, namely, the correlations of two degrees of freedom are taken into account, the critical velocity can also be determined by $\lim_{t \rightarrow \infty} \langle x_1(t) \rangle = 0$ and results in

$$v_0^c = -\frac{C_1(\infty)x_{10} + C_2(\infty)x_{20}}{C_3(\infty)\cos\theta + C_4(\infty)\sin\theta}, \quad (7)$$

where θ denotes the incident angle between the initial velocity and the x_1 -direction, hence $v_{10} = v_0\cos\theta$ and $v_{20} = v_0\sin\theta$.

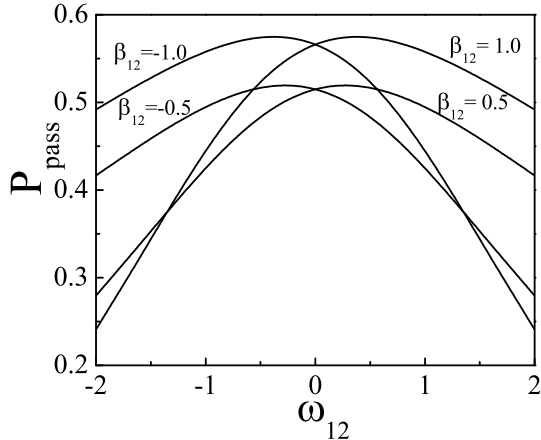


FIG. 2: The stationary passing probability as a function of the off-diagonal component ω_{12} for various β_{12} . The parameters used are the same as those in the figure 1.

Quantities plotted in the figures 1-7 are dimensionless and $k_B = 1.0$ except for the units having been included in the figure caption. In Fig. 1, we plot the critical velocity and the stationary passing probability as functions of the off-diagonal components of three coefficient tensors, where one of off-diagonal components varies and the other two are fixed to be zero. The stationary passing probability is calculated by $P_{\text{pass}} = \lim_{t \rightarrow \infty} \frac{1}{2} \text{erfc} [-\langle x_1(t) \rangle / (\sqrt{2} \sigma_{x_1}(t))]$. It is shown that the critical velocity increases with increasing the absolute value of m_{12} or ω_{12} ; while decreases with the increase of $|\beta_{12}|$. The larger critical velocity of a system needs, the more difficult for the particle is to arrive at the potential top. This also implies that the passing probability is small when the dissipation along the diffusive path is large if the potential differences between the saddle point and the initial positions are equivalent. As is shown in the figure, the behavior of the passing probability is opposite to that of the corresponding critical velocity.

Figure 2 shows the stationary passing probability in the presence of two off-diagonal components ω_{12} and β_{12} , simultaneously, for $m_{12} = 0$. It is seen that the maximum of the passing probability does not appear in the vertical case ($\omega_{12} = 0$). In the 2D PES, the particle is usually supposed to travel along the potential valley and then the steepest decedent direction. Because this is the direction which faces a smaller potential barrier. However, it may not be a path with a weaker damping. Under the effect of the off-diagonal component of the friction tensor, the particle is forced to select a better path with both low potential barrier and weak friction to surmount the saddle point of the potential.

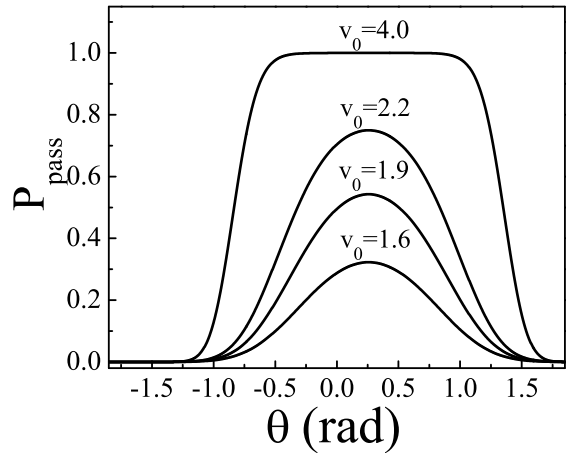


FIG. 3: The stationary passing probability as a function of the incident angle. Here $m_{12} = 0.6$, $\beta_{12} = 0.8$, and $\omega_{12} = -0.5$, as well as the other parameters are used as those in the figure 1.

B. Determination of the optimal path

Where is the optimal incident direction which enables the particle with given initial kinetic energy to have a larger passing probability? In order to determine this direction, we need to choose a special angle θ_m which enables the critical velocity to reach its minimum, i.e., from Eq. (7),

$$\left. \frac{dv_0^c}{d\theta} \right|_{\theta=\theta_m} = 0, \quad \theta_m = \arctan \left(\frac{C_4(\infty)}{C_3(\infty)} \right). \quad (8)$$

In fact, the largest analytically root of $P(s) = 0$ dominantly determines the passing probability. The optimal incident angle θ_m can then be expressed by the Langevin coefficients as

$$\theta_m = \arctan \left(\frac{m_{12}(\beta_{22}a + \omega_{22}) - m_{22}(\beta_{12}a + \omega_{12})}{m_{11}F_5(a) + m_{12}F_6(a)} \right). \quad (9)$$

Using the same parameters as those written in Figs. 1 and 3, we obtain $\theta_m \simeq 0.258$ rad, as is explicitly shown in Fig. 3, corresponding to the maximum of the stationary passing probability.

We now define γ , ψ and α to be the rotation angle of the major axis of the potential-curvature, friction and inertia tensors, respectively. They are found to have the following expressions:

$$\begin{aligned} \tan 2\gamma &= \frac{2\omega_{12}}{\omega_{22} - \omega_{11}}, & \tan 2\psi &= \frac{2\beta_{12}}{\beta_{22} - \beta_{11}}, \\ \tan 2\alpha &= \frac{2m_{12}}{m_{22} - m_{11}}. \end{aligned} \quad (10)$$

As an example, for the case we have studied in Figs. 1 and 3, these angles are: $\gamma \simeq -7.973^\circ$, $\psi \simeq -34.722^\circ$,

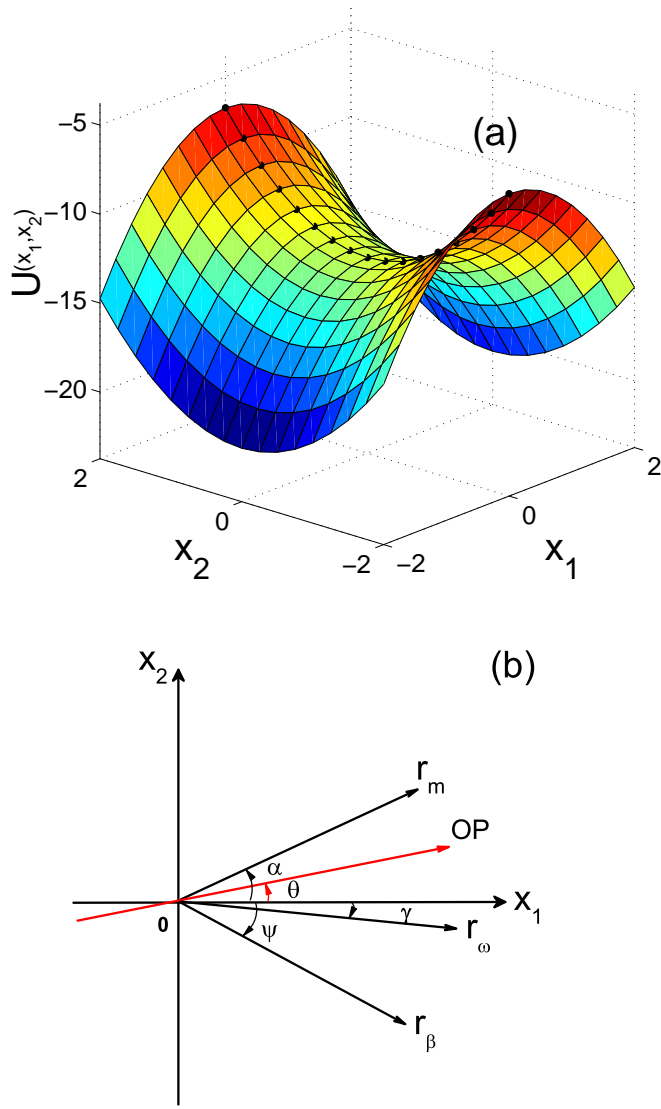


FIG. 4: (color online.) (a) The 2D potential energy surface, where the dotted curve is the saddle ridge line. (b) A schematic illustration of the optimal diffusion path (OP), where \mathbf{r}_m , \mathbf{r}_β , and \mathbf{r}_ω denote the major axes of the inertia, friction, and potential-curvature tensors, respectively.

and $\alpha \simeq 33.690^\circ$. For comparison, we write the optimal incident direction of the particle we have obtained in the unit of one degree, i.e., $\theta_m \simeq 14.779^\circ$ (0.258 rad).

In Fig. 4, we plot the two-dimensional quadratic potential and the optimal path in the x_1 - x_2 plane in a way of schematic illustration. All the coefficient elements used here have been written in the figures 1 and 3. It is illustrated that the direction of the optimal path departs from the x_1 -direction. The effect of off-diagonal component of the inertia tensor makes the average path of the diffusive system turn toward the positive x_2 -axis, while the off-diagonal component of friction leads the mean path of the particle toward the negative x_2 -axis. Finally, the

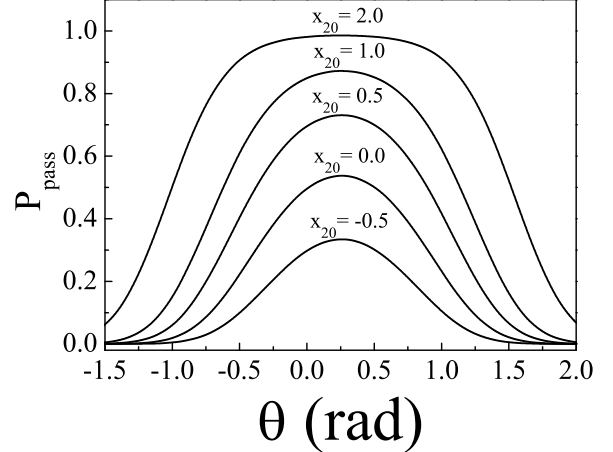


FIG. 5: The stationary passing probability as a function of θ for various x_{20} . Here $x_{10} = -1.0$, $v_0 = 1.9$, $m_{12} = 0.6$, $\beta_{12} = 0.8$, and $\omega_{12} = -0.5$, as well as the other parameters are the same as the figure 1.

competition of these two effects results in the optimal diffusive path shown in Fig. 4 (b). This phenomenon is similar to the quasi-stationary flow passing over the barrier in the fission case [15], where the magnitude of the current is strongly influenced by the off-diagonal components of inertia and friction tensors.

Figure 5 shows the dependence of the stationary passing probability on the incident angle of the particle starting from various initial positions but with fixed initial kinetic energy. It is seen that the passing probability of the particle starting from a large positive x_{20} position is larger than that of starting from both small and negative x_{20} positions. This is because the energy difference between the potential top and the initial position of the particle is small for the former. Amusingly, we find that the difference between the passing probabilities of two symmetrical positions ($-1.0, -0.5$) and ($-1.0, 0.5$) is observably large.

For a clearly understanding of the above results, we plot in Fig. 6 the mean diffusive path of a particle starting from different initial positions with different incident angles. Here $\langle x_1(t) \rangle$ has been obtained in Eq. (6) and

$$\langle x_2(t) \rangle = \sum_{i=1}^2 [C_{i+4}(t)x_{i0} + C_{i+6}(t)v_{i0}], \quad (11)$$

where all the time-dependent quantities are given in the appendix. The critical velocities are calculated by using Eq. (7): $v_0^c = 1.5791$ when $x_{20} = 0.5$; $v_0^c = 2.2321$ when $x_{20} = -0.5$, for $x_{10} = -1.0$ and $\theta = 0$. Hence the stationary passing probability of the particle starting from $x_{20} = 0.5$ is larger than that of the particle starting from $x_{20} = -0.5$. In particular, under the present

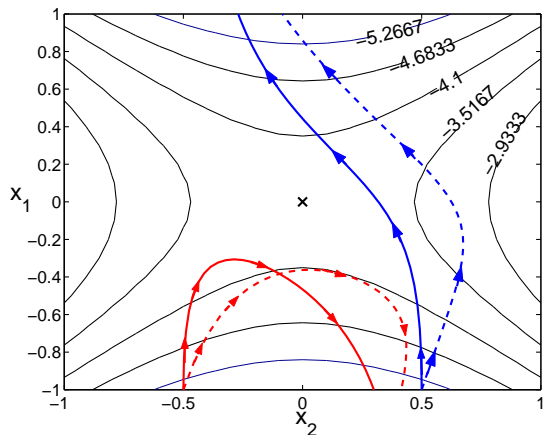


FIG. 6: (color online.) The mean diffusion path of a particle starting from the initial positions of two kinds at fixed $v_0 = 1.9$, where the solid and dashed lines correspond to $\theta = 0$ and $\theta = 0.258$ rad, respectively. Here all the Langevin parameters are the same as the figures 1 and 5.

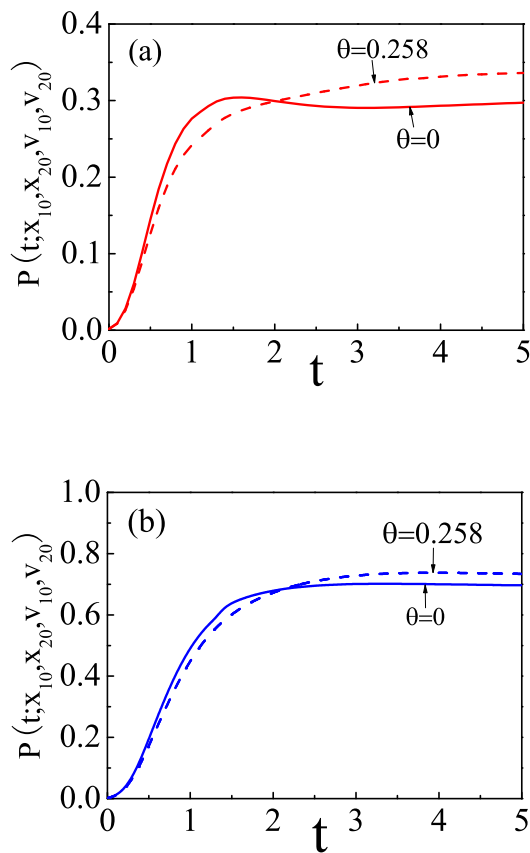


FIG. 7: (color online.) Time-dependent passing probability for various x_{20} and θ . Here $x_{10} = -1.0$, $v_0 = 1.9$, $x_{20} = -0.5$ in (a) and $x_{20} = 0.5$ in (b), as well as the Langevin parameters are the same as the figures 1 and 5.

circumstance, the diffusive process of the particle with different incident angles shows an interesting behavior. Because the initial velocity of the particle along the x_1 -direction for $\theta = 0$ is larger than that of $\theta = 0.258$ rad, the former can move to a position being closer to the saddle point than the latter. Thus the passing probability for $\theta = 0$ is larger than that of $\theta = 0.258$ rad at the beginning. However, the width of the Gaussian distribution is independent of the incident angle and increases with the increase of time. Although the center position of the particle's distribution with $\theta = 0.258$ rad is behind that of $\theta = 0$, as the time goes on, it will have a larger share of distribution passed the saddle point. Therefore, the passing probability for a particle with incident angle $\theta = 0.258$ rad is larger than that of $\theta = 0$ in the long time.

Time-dependent passing probabilities shown in Figs. 7 (a) and 7 (b) are also in complete agreement with the above theoretical analysis.

IV. APPLICATION TO FUSION OF MASSIVE NUCLEI

We now apply the present 2D simplified diffusive model to investigate the fusion of two massive nuclei, which has been described by directional diffusion over the saddle point [6]. As a particular example, we calculate the fusion probability of the nearly symmetrical reaction system $^{100}\text{Mo} + ^{110}\text{Pd}$ [16], which is plotted as a function of the center-of-mass energy $E_{c.m.}$ in Fig. 8. A schematic illustration of the deformation of the compound nucleus is also shown in this figure. The temperature of the fusing system is determined by $aT^2 = E_{c.m.} + Q - E_B$, where $a = A/10$ is the energy level constant with A the nucleon number of the compound nucleus, Q denotes the reaction Q value and E_B the barrier height of fission potential.

The $\{c, h, \alpha\}$ shape parametrization [17] with the elongation c (the half of the nuclear length) and neck variable h are used, i.e, $x_1 = c$, $x_2 = h$, and the asymmetrical parameter α is fixed to be zero. The inertia and friction tensors are calculated by the Werner-Wheeler method and the one-body dissipative mechanism [18], respectively, all the Langevin coefficients are considered to be constants at the saddle point. The three components of potential-curvature tensor are: $\omega_{11} = -28.2304$, $\omega_{22} = 275.4211$, and $\omega_{12} = 50.4551$ in the unit of MeV; the components of friction tensor $\beta_{11} = 701.9967$, $\beta_{22} = 621.4425$, $\beta_{12} = 601.4934$ in the unit of 10^{-21} MeV-sec; the inertia elements $m_{11} = 102.4081$, $m_{22} = 134.4673$, and $m_{12} = 110.3783$ in the unit of 10^{-42} MeV-sec².

It is found a highlighted interesting result from Fig. 8 that there exists the optimal collision shape for projectile and target nuclei, which induces the maximum fusion probability under the same center-of-mass energy. It can be easily understood from a combining role of the off-diagonal components of three dynamical coefficient tensors. This concludes that the fusion probability of mas-

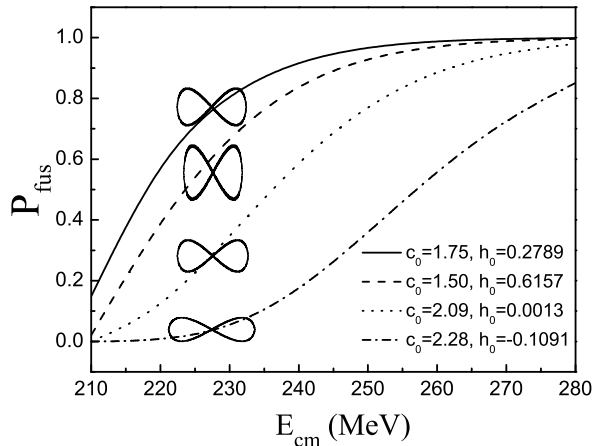


FIG. 8: The fusion probability of the reaction $^{100}\text{Mo} + ^{110}\text{Pd}$ as a function of the center-of-mass energy for various initial positions. Schematically illustrated as well are the deformed shape of the compound nucleus.

sive nuclei can be enhanced if the two collision heavy ions are polarized to be ellipsoid and the collision direction between the long and short axis of ellipsoid is appropriately selected. For the fusion of deformed massive nuclei, there exists the optimal angle for the incident nucleus to collide with the target one, which favors the fusion of heavy ions to be accomplished.

Figure 9 shows the fusion probability of $^{100}\text{Mo} + ^{110}\text{Pd}$ as a function of the center-of-mass energy when the off-diagonal components are considered partly. Here the initial position of the fusing system is chosen into the optimal one, i.e., $c_0 = 1.75$ and $h_0 = 0.2789$ as well as all the parameters used are the same as the figure 8. This fusion reaction system is regarded as an example to compare the results with and without off-diagonal components in the potential surface, friction and mass parameters, which is reflected in the result presented in the above section. In fact, the case of without all off-diagonal components is equivalent to the one dimension or without the neck situation [4].

It is seen from Fig. 9 that the increase of the 1D fusion probability curve versus the energy is faster than that of 2D case. It has been known that the pervious 1D diffusion model without the neck variable proposed the fusion probability larger than the experimental data, so the present completely coupled 2D diffusion model might be appropriate. Moreover, the results for the presence of only one of three off-diagonal components can also be understood from the critical velocity (kinetic energy), to see Fig. 1. Namely, the larger the critical kinetic energy of the system is, the less the fusion probability is for the same center-of-mass energy. The nonvanishing β_{12} allows the smallest critical kinetic energy and the

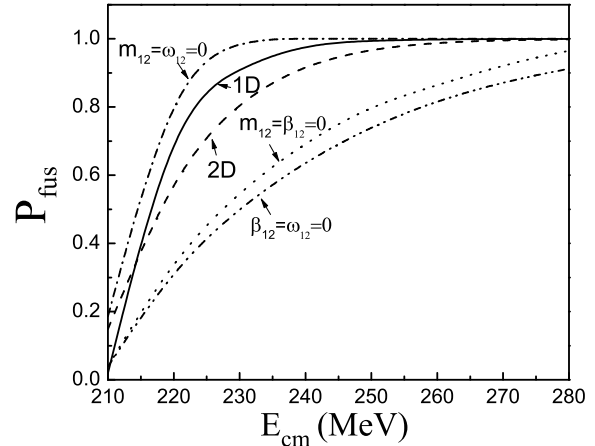


FIG. 9: The fusion probability of the reaction $^{100}\text{Mo} + ^{110}\text{Pd}$ as a function of the center-of-mass energy for the situations with and without off-diagonal components.

presence of m_{12} leads to the largest critical kinetic energy. Therefore, we have a relation for the fusion probabilities: $P_{\text{fus}}(\beta_{12} \neq 0) > P_{\text{fus}}(\omega_{12} \neq 0) > P_{\text{fus}}(m_{12} \neq 0)$ at a fixed center-of-mass energy.

V. SUMMARY

We have studied the diffusion process of a particle passing over the saddle point of a two-dimensional non-orthogonal quadratic potential. The expression of the passing probability is obtained analytically, where the inertia and friction tensors are not diagonal. The optimal incident angle of the particle's initial velocity is determined. Our results have shown that the optimal diffusive path, which departs from the potential valley in the two-dimensional potential energy surface, induces the maximum saddle-point passing probability. This is due to the competition effect between the off-diagonal components of inertia, friction and potential-curvature tensors. We have investigated the fusion probability of massive nuclei and compared the results with and without off-diagonal terms, for instance, the reaction of $^{100}\text{Mo} + ^{110}\text{Pd}$. Due to the influences of off-diagonal components of inertia and friction upon the diffusive path, which are calculated by the $\{c, h, \alpha\}$ parametrization, the fusion probability can be enhanced for an appropriate choice of the collision direction of the deformable target and projectile nuclei. The optimal configurations of colliding nuclei is between spherical and extremely deformed ones. In further, the present study also provides useful information in connection with the synthesis of superheavy elements.

ACKNOWLEDGEMENTS

This work was supported by the National Natural Science Foundation of China under Grant Nos. 10674016, 10747166 and the Specialized Research Foundation for the Doctoral Program of Higher Education under Grant No. 20050027001.

APPENDIX. THE EXPRESSIONS OF $\langle x_1(t) \rangle$ AND $\langle x_2(t) \rangle$

The quantities appear in the expression of $\langle x_1(t) \rangle$ are

$$\begin{aligned}
 P(s) &= (\det m)s^4 + (m_{11}\beta_{22} + m_{22}\beta_{11} - 2m_{12}\beta_{12})s^3 \\
 &\quad + (\det\beta + m_{11}\omega_{22} + m_{22}\omega_{11} - 2m_{12}\omega_{12})s^2 \\
 &\quad + (\beta_{11}\omega_{22} + \beta_{22}\omega_{11} - 2\beta_{12}\omega_{12})s + \det\omega, \\
 F_1(s) &= (\det m)s^3 + (m_{11}\beta_{22} + m_{22}\beta_{11} - 2m_{12}\beta_{12})s^2 \\
 &\quad + (\det\beta + m_{11}\omega_{22} - m_{12}\omega_{12})s + \beta_{11}\omega_{22} - \beta_{12}\omega_{12}, \\
 F_2(s) &= (m_{12}\omega_{22} - m_{22}\omega_{12})s + \beta_{12}\omega_{22} - \beta_{22}\omega_{12}, \\
 F_3(s) &= (\det m)s^2 + (m_{11}\beta_{22} - m_{12}\beta_{12})s + m_{11}\omega_{22} \\
 &\quad - m_{12}\omega_{12}, \\
 F_4(s) &= (m_{12}\beta_{22} - m_{22}\beta_{12})s + m_{12}\omega_{22} - m_{22}\omega_{12}, \\
 F_5(s) &= m_{22}s^2 + \beta_{22}s + \omega_{22}, \\
 F_6(s) &= -m_{12}s^2 - \beta_{12}s - \omega_{12},
 \end{aligned} \tag{12}$$

where $\det m = m_{11}m_{12} - m_{12}^2$ and $\det\beta = \beta_{11}\beta_{22} - \beta_{12}^2$.

The time-dependent factors in the expression of $\langle x_2(t) \rangle$ in Eq. (11) read $C_j(t) = L^{-1}[F_{j+2}(s)/P(s)]$ ($j = 5, \dots, 8$) being resulted from the inverse Laplace transforms, as well as

$$\begin{aligned}
 F_7(s) &= (m_{12}\omega_{11} - m_{11}\omega_{12})s + \beta_{12}\omega_{11} - \beta_{11}\omega_{12}, \\
 F_8(s) &= (\det m)s^3 + (m_{11}\beta_{22} + m_{22}\beta_{11} - 2m_{12}\beta_{12})s^2 \\
 &\quad + (m_{22}\omega_{11} - m_{12}\omega_{12} + \det\beta)s + \beta_{22}\omega_{11} \\
 &\quad - \beta_{12}\omega_{12}, \\
 F_9(s) &= (m_{12}\beta_{11} - m_{11}\beta_{12})s + m_{12}\omega_{11} - m_{11}\omega_{12}, \\
 F_{10}(s) &= (\det m)s^2 + (m_{22}\beta_{11} - m_{12}\beta_{12})s + m_{22}\omega_{11} \\
 &\quad - m_{12}\omega_{12}.
 \end{aligned} \tag{13}$$

-
- [1] H. Hofmann and R. Samhammer, *Z. Phys. A* **322**, 157 (1985).
- [2] Y. Aritomo, T. Wada, M. Ohta, and Y. Abe, *Phys. Rev. C* **55**, R1011 (1997); **59**, 796 (1999); Y. Abe, Y. Aritomo, T. Wada, and M. Ohta, *J. Phys. G* **23**, 1275 (1997).
- [3] W. J. Świątecki, K. Siwek-Wilczyńska, and J. Wilczyński, *Phys. Rev. C* **71**, 014602 (2005).
- [4] C. E. Aguiar, V. C. Barbosa, R. Donangelo, and S. R. Souza, *Nucl. Phys. A* **491**, 301 (1989).
- [5] C. E. Aguiar, V. C. Barbosa, and R. Donangelo, *Nucl. Phys. A* **517**, 205 (1990).
- [6] Y. Abe, D. Boilley, B. G. Giraud, and T. Wada, *Phys. Rev. E* **61**, 1125 (2000).
- [7] J. D. Bao and D. Boilley, *Nucl. Phys. A* **707**, 47 (2002).
- [8] N. Takigawa, S. Ayik, K. Washiyama, and S. Kimura, *Phys. Rev. C* **69**, 054605 (2004).
- [9] S. Ayik, B. Yilmaz, A. Gokalp, O. Yilmaz, and N. Takigawa, *Phys. Rev. C* **71**, 054611 (2005).
- [10] D. Boilley, Y. Abe, and J. D. Bao, *Europhys. J. A* **18**, 627 (2003).
- [11] J. D. Bao and Y. Z. Zhuo, *Phys. Rev. C* **67**, 064606 (2003).
- [12] C. R. Morton, A. C. Berriman, R. D. Butt, M. Dasgupta, D. J. Hinde, A. Godley, and J. O. Newton, *Phys. Rev. C* **64**, 034604 (2001).
- [13] I. I. Gontchar, M. Dasgupta, D. J. Hinde, R. D. Butt, and A. Mukherjee, *Phys. Rev. C* **65**, 034610 (2002).
- [14] I. I. Gontchar, D. J. Hinde, M. Dasgupta, C. R. Morton, and J. O. Newton, *Phys. Rev. C* **73**, 034610 (2006).
- [15] J. S. Zhang and H. A. Weidenmüller, *Phys. Rev. C* **28**, 2190 (1983).
- [16] K.-H. Schmidt and W. Morawek, *Rep. Prog. Phys.* **54**, 949 (1991).
- [17] M. Brack, J. Damgaard, A. S. Jensen, H. C. Pauli, V. M. Strutinsky, and C. Y. Wong, *Rev. Mod. Phys.* **44**, 320 (1972).
- [18] Y. Jia and J. D. Bao, *Phys. Rev. C* **75**, 034601 (2007).